Impinging Streams of Hypergolic Propellants," TM 33-395, July 15, 1968, Jet Propulsion Lab., Pasadena, Calif.

[6] Lawver, B. R., "An Experimental Study of N_2O_4/N_2H_4 Jet Separation Phenomena," Paper presented at the Fifth ICRPG Combustion Conference, Baltimore, Md., Oct. 1968.

[7] Priem, R. J. and Heidmann, M. F., "Propellant Vaporization as a Design Criteria for Rocket Engine Combustion Chambers," TR R-67, 1960, NASA.

[8] Anderson, R. E., "A Model for N_2O_4 Rich Reactions," Technical Paper 3 LRO, Dec. 1964, Aerojet General Corp., Sacramento, Calif.

[9] Beltran, M. R. et. al., "Liquid Rocket Engine Combustion Instability Studies," AFRPG TR 66-125, July 1966, Dynamic Science Corp., Monrovia, Calif.

[10] Dickerson, R., Tate, K., and Parsec, N., "Correlation of Spray Injector Parameters with Rocket Engine Performance," AFRPL TR 68-147, June 1968, Edwards, Calif.

[11] Matthews, B. J., Wuerken, R. F., and Harje, D. T., "Small Droplet Measuring Technique," AFRPL TR-68-156, Edwards, Calif.

[12] Kliegel, J. R. et al., "Two Dimensional Kinetic Nozzle Analysis Computer Program," AD 841200, July 1968, ICRPG Performance Standardization Working Group.

[13] Weingold, H. D. and Zupnik, T. F., "Turbulent Boundary Layer Nozzle Analysis Computer Program-TBL," AD 841202, July 1968, ICRPG Performance Standardization Working Group.

[14] Frey, H. M. et al., "One Dimensional Kinetic Nozzle Analysis Computer Program," AD 841201, July 1968, ICRPG Performance Standardization Working Group.

OCTOBER 1969 J. SPACECRAFT VOL. 6, NO. 10

Saturn V/S-IC Stage Base Thermal Environment

C. R. MULLEN* AND R. L. BENDER†
The Boeing Company, Huntsville, Ala.

This paper contains an analysis of the measured thermal and pressure environments in the base of the S-IC stage during the AS-501 and AS-502 flight tests. Base gas temperatures, radiation levels, and total heating rates were measured during both flights and base-mounted TV cameras on the AS-502 flight provided a visual observation of the base gas flowfield. These data indicate that significant radiation is contributed by hot gases being recirculated into the base. Radiation was the main source of heating, although convective heating on the engine nozzle extension was significant. Base flow deflectors on the AS-501 flight were removed for the AS-502 flight and produced a significant increase in AS-502 base heating. Comparisons of flight data with model test data indicate that model data are useful in defining base pressure, gas temperature, and effects of changing configuration but cannot be used directly to indicate magnitudes of convective or radiation heating for the prototype.

Introduction

THE Saturn V booster is the largest of the Saturn class vehicles developed by NASA/MSFC to implement the Apollo moon landing program. One of the areas of concern during the design and development of the Saturn V was the base region of the S-IC stage where significant heating was expected to occur during boost. A part of the Saturn V/S-IC stage development program conducted by The Boeing Company and NASA/Marshall Space Flight Center consisted of extensive base heating model tests, application of Saturn I and IB flight test data[1] and instrumenting of the first Saturn V flight vehicles to define the S-IC base environment to assure adequate base thermal protection.

The AS-501 and AS-502 flights on November 9, 1967 and April 4, 1968, respectively, produced a significant amount of S-IC base heating data.[2,3] The Saturn V/S-IC stage base configuration consists of five F-1 engines mounted in a cross-engine arrangement of four maneuverable engines around a fixed center engine (Figs. 1). The engines use LOX/RP-1 at a mixture ratio of 2.26:1. A heat shield is located 19 ft forward of the engine exits and base flow deflectors were located on the AS-501 around the periphery of the base to remove combustible gas mixtures from the base area and to cool the base. The flow deflectors were removed on AS-502. Turbopump exhaust gases were eliminated by exhausting them inside the F-1 engine nozzle from the 10:1 to 16:1 area ratio. This created a fuel rich gas mixture surrounding each of the engine exhaust flows. This paper describes the measured S-IC base heating environments and compares them with Saturn I and IB flight data and 1/45th-scale model test data.

Presented as Paper 69-318 at the AIAA 3rd Flight Test, Simulation, and Support Conference, Houston, Texas, March 10–12, 1969; submitted February 28, 1969; revision received July 1, 1969.

* Senior Group Engineer, Aerophysics. Member AIAA.
† Member of Aerophysics Group. Member AIAA.

Flight Instrumentation and Data Reduction

The instrumentation consisted of 6 radiation calorimeters, 19 total calorimeters, 14 gas temperature probes, 18 static pressure taps, 4 total pressure probes, and 2 differential pressure gages at the locations shown in Fig. 1.

The sensing surfaces of the heat shield total and radiation calorimeters were 0.17 in. and 0.55 in. in diameter, respectively, and were mounted so that the sensing surfaces of the total calorimeters and the sapphire windows of the radiation calorimeters were flush with the heat shield surface. The sapphire window on the radiation gage was protected from sooting by a nitrogen purge. The radiation and total calorimeters are asymptotic instruments with a constantan sensor surface coated with a high-emissivity black coating.[4,5] The calorimeters maintained a low wall temperature throughout flight with an "effective"[6] sensing surface temperature of approximately 610°R.

The heat shield gas temperature probes consisted of a 0.25-in. diam molybdenum single shield with a platinum rhodium thermocouple junction for the sensing surface. Gases were admitted to the sensing surface through four equally spaced

openings facing parallel to the heat shield. The sensors were mounted 0.25, 1.00, and 2.50 in. aft of the heat shield surface.

Each F-1 engine was enclosed in a "cocoon" which consisted of fibrous silica insulation enclosed in inconel foil, except for the nozzle extension where wire reinforced asbestos was used as shown in Fig. 2. Engine instrumentation protruded above the smooth surfaces of the engine and the cocoon insulation was contoured to enclose the transducers and was flush with the sensing surfaces of the instruments. The engine calorimeters were the same type as that used for the heat shield. The engine gas temperature probes were different from the heat shield, consisting of a double platinum shield and a platinum-platinum rhodium thermocouple. Gases were admitted to the thermocouple through offset openings in both the inner and outer shields.

Two TV cameras were mounted in the S-IC thrust frame compartment, near position I and position III, just forward of the heat shield. Data were taken several seconds before liftoff until after S-IC/S-II stage separation. Each camera was equipped with two flexible fiber optic bundles, which extended through the heat shield, providing two fields of view from each camera (see Fig. 3). The camera lenses were continuously rotated during flight to remove carbon deposits. The TV pictures provided clear evidence of local base area insulation failures and the advent of recirculated F-1 engine exhaust flow.

Raw data were transmitted on PAM/FM/FM and PCM/FM telemetry channels, with the majority of the data transmitted on PAM/FM/FM. The data were sampled 12 times per second and then calibrated, time edited, and interpolated to 10 samples per second (SPS). The data edit routine replaced data values which differed more than 2.5 standard deviations from the data set. The edited data were then filtered with a low band pass filter with the mean values of the data preserved during the filtering process.[7]

Flight Results

Base Flowfield

During the early period of boost, freestream air is drawn into the vehicle base by the aspirating effect of the engine exhaust flow. The heating during this period of flight is primarily radiation from the downstream plumes; it decreases as the plume pressure and emissivity decrease with altitude. At the higher altitudes, reversed flow of the lower energy exhaust gases occurs due to the expansion and interaction of the jet plumes. The recirculated gases flowing over the engine and heat shield surfaces created a convective heating environment for all surfaces cooler than the hot gas. This convective heating decreases at still higher altitudes because of the low density. The flight data have revealed that the hot carbon-laden gases in the S-IC base region also contribute significant radiation heating to the base region surfaces during the time of full recirculation.

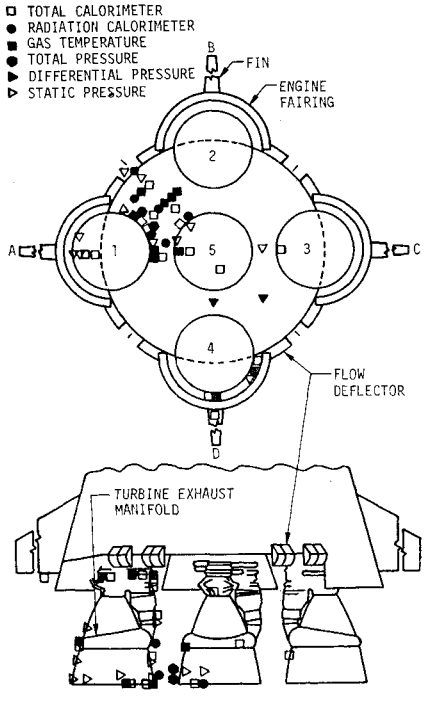

Fig. 1 Saturn V/S-IC heat shield and engine instrumentation.

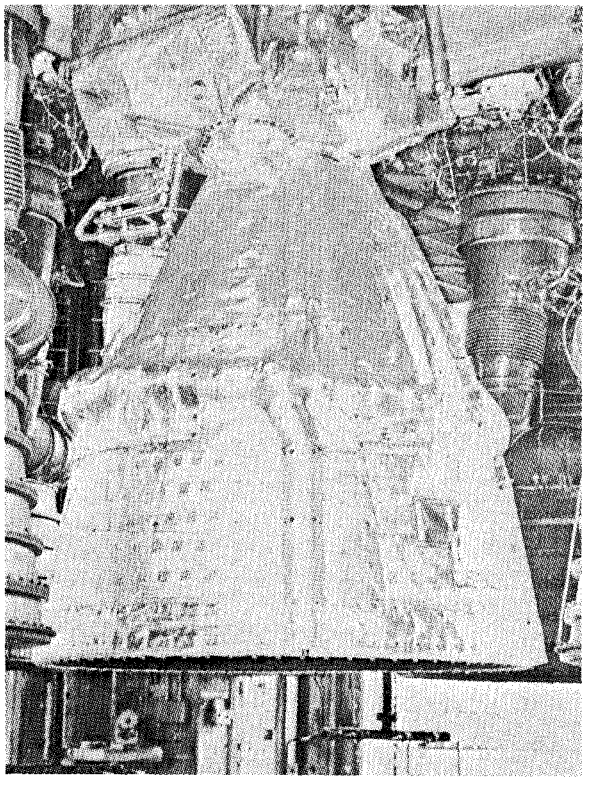

Fig. 2 S-IC stage center F-1 engine with insulation cocoon.

Above 80 kft, the highly expanded plumes cause boundary-layer flow separation over the aft end of the S-IC stage. This phenomenon was observed by ground tracking cameras. Base gases are fed into the separated region around the periphery of the base. Center engine shutdown, which occurs near the end of the first stage boost, causes a 3- to 5-sec transient in the base flowfield and heating environment.

Typical Base Heating and Pressure

Typical radiation ($\dot{q}_r$) and total ($\dot{q}_t$) heating rates and base gas temperatures (Tg) for the AS-501 and AS-502 flights are shown in Figs. 4–6. The radiation at sea level was about as expected based on analytical calculations. The radiation was then expected to decrease with increasing altitude but a sharp rise in radiation is noted which peaks between 60 kft and 100 kft. (This radiation hump is discussed in detail later.)

It is evident that the AS-502 base environment was more severe than that on AS-501 and will be discussed later. Maximum total and radiation heating rates measured on the base heat shield are 22 and 20 Btu/ft²sec, respectively, occurring at approximately 65 kft (Fig. 4). Maximum total and radiation heating rates to the engines are 32 and 27 Btu/ft²sec, respectively, occurring at approximately 50 kft (Fig. 5).

The difference between $\dot{q}_t$ and $\dot{q}_r$ for the heat shield indicates that a convective cooling rate was experienced by the calo-

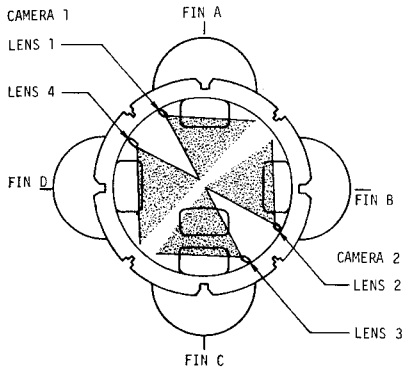

Fig. 3 Location and view of S-IC base region television cameras.

rimeters to approximately 30 kft. Small convective heating rates occurred from 30 kft through the remainder of first stage boost. Convective heating to the engine extensions occurred from liftoff throughout flight, with a sharp increase at 30 kft and peak values occurring between 40 and 60 kft. Convective heating rates from 2 to 14 Btu/ft²sec were experienced on the heat shield and engines.

Gas temperatures near the base reached a maximum between 60 and 75 kft. Gas temperatures near the engine exit plane began to rise immediately after liftoff, reached a maximum between 60 and 82 kft, and were approximately constant through the remainder of boost. The maximum measured gas temperatures on the heat shield and engines are 2100° and 2700°R, respectively.

The spikes in the heating environment shown in Fig. 6 at 162 and 185 kft are caused by center engine cutoff (CECO). CECO occurs at 162 and 185 kft for the AS-501 and AS-502, respectively, with outboard engine cutoff occurring at 207 and 196 kft. The TV camera data indicate a bright flash at CECO. The center engine cuts off fuel rich which increases the carbon concentration and consequently the base gas emissivity. Burning of fuel rich exhaust products is not expected to occur at these altitudes.

The heat shield and engine insulation surface temperature may be significantly higher than the effective calorimeter temperature, because of high radiant heating, and may also be higher than the gas temperature during part of boost as shown in Fig. 7. References to convective heating or cooling in this paper refer to calorimeter surfaces, and are not necessarily applicable to the heat shield or engine insulation.

Figure 8 shows that below 20 kft, freestream flow and engine aspiration reduce the base pressure below ambient. Plume expansion and impingement at the higher altitudes, and subsequent hot gas recirculation into the base increase base pressures above ambient.

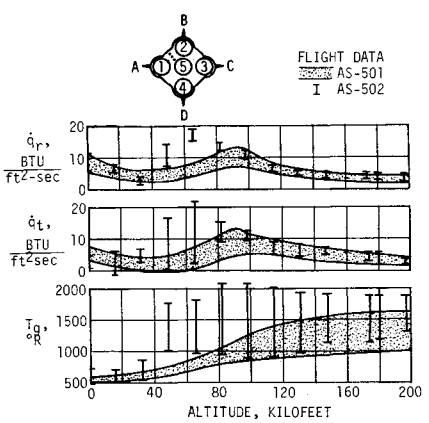

Fig. 4 AS-501 and AS-502 heat shield environment.

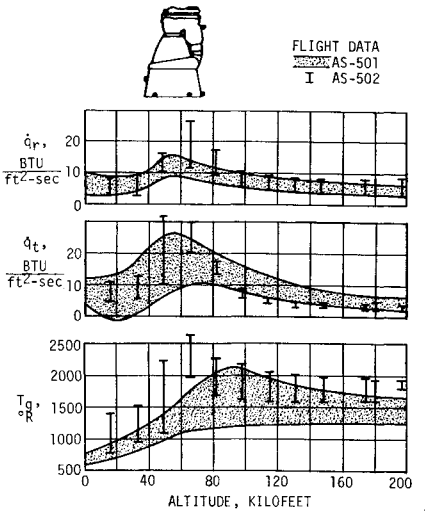

Fig. 5 AS-501 and AS-502 engine environment.

Radiation Hump

The flowfield visualization provided by the TV cameras on AS-502 was extremely important because of the correlations which were possible with flight data from the heat shield and engine instrumentation. The TV data show hot gases reaching the base heat shield at 40 kft which correlates with the rise in $\dot{q}_r$ on the heat shield as shown in Fig. 9. The arrival of hot recirculated gases in the base area is accompanied by radiation increases on all base and engine calorimeters. The TV data also show, that after 118 kft, the base region is clear, indicating a significant reduction in density (emissivity) of the hot gases. The clearing in the base correlates with the reduction in the measured heating rates.

Figure 9 also shows that the engine radiation starts to increase and peaks before the heat shield radiation and that the heat shield radiation starts and peaks before the fin-base heating. Once the radiation heating to these components peaks, the radiation heating to all components is nearly the same at all locations which would occur if all instruments were completely engulfed in gases of about the same temperature and emissivity. Figure 10 shows that Saturn I experiences a similar radiation hump although it appears to be less pronounced because of larger sea-level radiation. The AS-502 radiation peaks earlier and at higher magnitudes than AS-501. The peaks for both the Saturn V and Saturn I correspond closely with the time of maximum measured base gas temperature, and the gas temperatures are similar.

Since it appeared that hot gas recirculation caused the radiation hump, a simplified calculation was made to determine

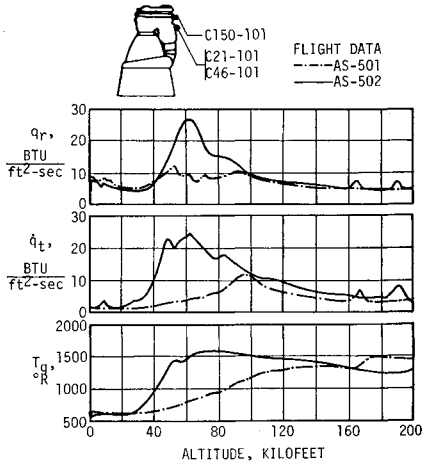

Fig. 6 Outboard engine environment—forward area.

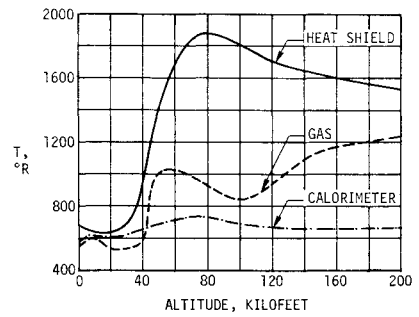

Fig. 7 Comparison of heat shield and calorimeter temperature with base gas temperature.

whether the base region gases possessed the necessary radiation potential. The calculation was made using measured gas temperature data and assuming the gas emissivity and view factor each to be unity. It can be seen from Fig. 11 that the total hot gases at the heat shield surface are not at sufficiently high temperatures to produce the measured radiation. However, gas temperatures measured around the F-1 engines do have the potential to produce the measured heating levels.

A detailed analytical calculation[8] of radiation from the exhaust plumes to the base of the fin was performed to determine whether the expansion of the plumes and the diminishing plume afterburning could cause the radiation hump. Calculations were made at various altitudes between 15 and 180 kft, using plume boundaries from AS-502 optical tracking data, and with and without carbon particles distributed through the plume. The results (Fig. 12) indicate that the radiation hump cannot be produced by the expansion and afterburning of the plume. The radiation prediction continues to diminish with increase in altitude.

The understanding of the source of radiation to the base areas of the Saturn V/S-IC has been increased significantly through the flight evaluation efforts on AS-501 and AS-502. It has been determined that maximum values of radiation do not occur at sea level, but instead result from recirculated gases present in the base region at higher altitudes. Based upon flight data, it is also evident that the earlier the gases are present in the base, the higher will be the temperature; and, consequently, higher radiation will result. The ability to predict the radiation hump analytically, however, is seriously limited and requires additional development of analytical tools.

Base Flow Deflector Effects

The flow deflectors which were on the AS-501 flight vehicle to remove combustible hot gas mixtures from the base area were removed on the AS-502 vehicle, since the measured base environment on the AS-501 was well below design limits. The comparison of AS-501 and AS-502 flight data on the heat shield and center engine, Figs. 4 and 5, respectively, show that significant differences do exist with radiation and total heating peaking higher and earlier for the AS-502 than for the AS-501. It was expected that flow deflectors would only affect the

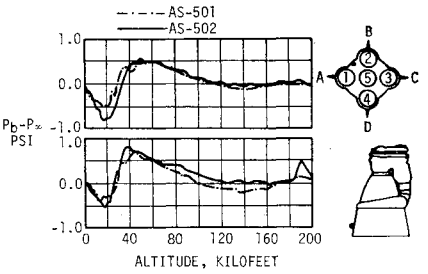

Fig. 8 Typical AS-501 and AS-502 base pressures.

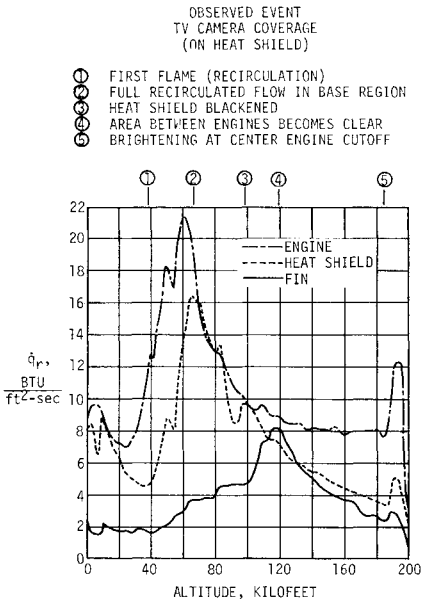

Fig. 9 Comparison of radiation to engine, heat shield and fin.

convective heating; but because of the unexpected radiation from the recirculated exhaust gases in the base region, radiation was the heating mechanism most affected.

Engine areas near the exit plane were not as significantly affected by the flow deflectors as the heat shield (Fig. 5). Outboard locations, such as the outboard surfaces of the outboard engine and the base of the fins, were not expected to experience significant flowfield or heating changes when the deflectors were removed. The comparison of flight data to the base of the fin in Fig. 12 shows similar environments for both flights. It is also noted in Fig. 12 that the first rise in the fin heating corresponds to the time of arrival of the recirculated gases as noted by the TV camera, and the second more rapid rise corresponds to the time of plume induced flow separation. The AS-501 base pressures on the heat shield shown in Fig. 8 were higher in the 10 to 40 kft altitude regime than on AS-502 which is attributed to the flow deflector removal on AS-502. Flow deflectors, however, did not affect the engine external surface pressures.

It was concluded that the differences between the AS-501 and AS-502 flight data were almost entirely due to flow deflector effects. Subsequent flight data have also confirmed this conclusion.

Environmental Effects

The S-IC heat shield and engine insulation were adequate to maintain structural temperatures below design limits. The base TV cameras on the AS-502 vehicle indicated that the M-31 insulation on the heat shield was cracking and pieces were falling from the base. This increased structural temperature in local areas but was not prohibitive.

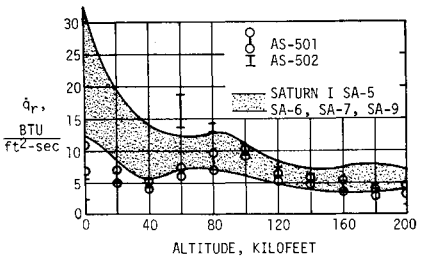

Fig. 10 Comparison of Saturn I and Saturn V heat shield radiation.

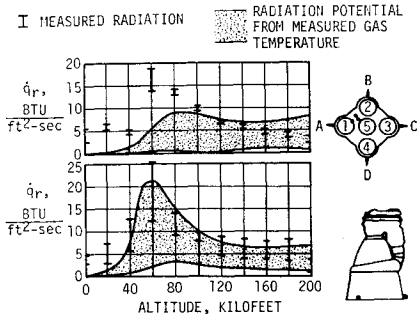

Fig. 11 Comparisons of radiation data with radiation potential—heat shield and engines.

Experimental Model Data

A model test program was initiated early in 1962 to help define base heating environments on the Saturn V/S-IC stage. A short-duration test technique[9] was used because it provided a much cheaper and simpler method of testing. Run times were in the order of 8 to 10 msec. Confidence in the technique was obtained when S-I short-duration model base heating compared favorably with existing longer-duration model test data. A $\frac{1}{45}$th scale model of the S-IC base regions was designed by Cornell Aeronautical Laboratory (CAL) and fabricated by the NASA/Marshall Space Flight Center.

Tests were conducted in CAL's high-altitude chamber at altitudes between 125 and 205 kft with no external flow and in the CAL transonic tunnel between Mach 0.6 and 1.2. The Lewis Research Center transonic and supersonic wind tunnels were used to produce model data in the Mach 0.4 to 3.5 range. The model used GOX/Ethylene to simulate LOX/RP-1. Hydrogen was used in the model to simulate the turbine exhaust which is injected into the main exhaust flow inside each of the nozzles at the 10:1 area ratio.

Thin film heat-transfer gages were employed for the measurement of short-duration heating. Heat-transfer gages are constructed to allow measurement of radiant and total heating rates. Because of the short time duration of the model test, the gages are recording a cold wall heating rate similar to the flight instrumentation. Short-duration surface pressure measurements are made on the model base using CAL developed piezoelectric pressure transducers.

Comparison of Flight and Model Data

Because of the size of the Saturn V, small scale models were required for model testing. The $\frac{1}{45}$th scale model was selected for the short-duration tests to meet the wind-tunnel and altitude chamber size requirements. This small model created heating environments[10] which contained significant scaling effects. The total heating environment is composed of radiation and convective heating, both of which are dependent on flowfield size.

If similarity is obtained between the model exhaust gases and the flight vehicle exhaust gases, radiation is expected to increase with increase in size such that the flight vehicle radiation is significantly higher than the model. However, the model exhaust gases were not similar to the full scale (GOX/Ethylene gas was used in the model to simulate LOX/RP-1) and did not produce sufficient carbon in the plume or in the recirculated gases to maintain correct similarity of emissivity with a LOX/RP-1 plume. This lower emissivity, combined with a small radiating gas source, resulted in negligible radiation heating to the model heat shield and engines, as shown in the upper comparisons of Figs. 13 and 14.

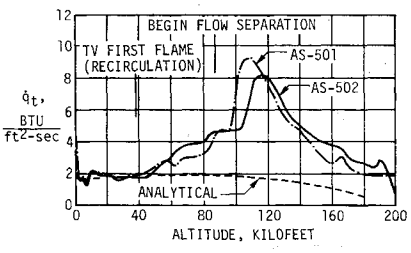

Fig. 12 Base of fin environment.

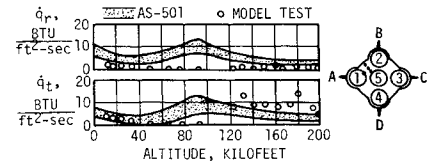

Fig. 13 Comparison of model and flight data heating rates—heat shield.

Convective heating in the base is a function of the running length and is affected by relative size. The smaller the running length, the larger the convective heating and, consequently, the convective heating on the model was expected to be much larger than that experienced on the flight vehicle. Model total heating rate data, shown in the lower comparisons of Figs. 13 and 14, are almost totally made up of convective heating and follows the expected trend. The model convective heating is observed to be much greater than the flight data (subtract upper band from lower band, Fig. 13). The model convective heating data did indicate the trends (increases and decreases) in the environment with configuration changes such as shortening the fairings, removing the flow deflectors, or gimbaling the outboard engines. A good example is the increase in base and center engine heating with the removal of flow deflectors which was indicated by the model data and verified with the AS-502 flight data.

Base pressure measurements from model and flight tests are compared in Fig. 15. The shapes of the curves are very similar but the flight data rise more rapidly in the 30–60 kft range.

Flight and model base gas temperatures are compared in Fig. 16. The flight data show large gradients in gas temperature near the heat shield and the accuracy of the model data is not good but it is evident that the flight and model data have comparable magnitudes of gas temperature at the higher altitudes. It was concluded that the model data were useful in defining magnitude and trends in the base pressure and gas temperature but could not be used directly to indicate magnitudes of convective or radiation heating.

Additional development of the model testing technique is required to obtain better simulation of the LOX/RP-1 exhaust gases. With the added information from Saturn V full-scale test data which indicates that recirculating hot gases can contribute significantly to base radiation, it is presently more accurate to predict analytical base radiation using existing flight data and full-scale sea level radiation measurements than to use model test results. Model testing is still a requirement, however, to predict when hot gases would be expected in the base region, to indicate magnitudes of base pressure and base gas temperature, and to determine relative heating effects with changes in configuration.

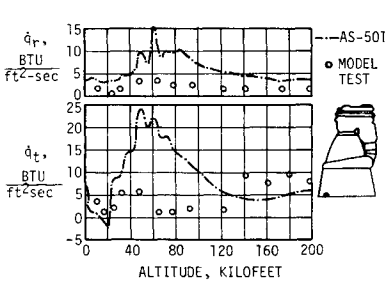

Fig. 14 Comparison of model and flight data heating rates—center engine.

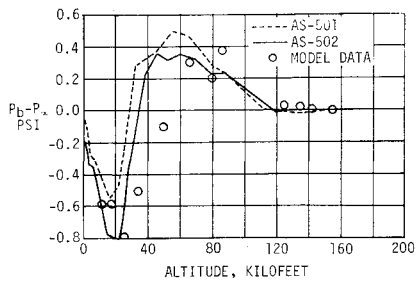

Fig. 15 Comparison of model and flight data base pressure.

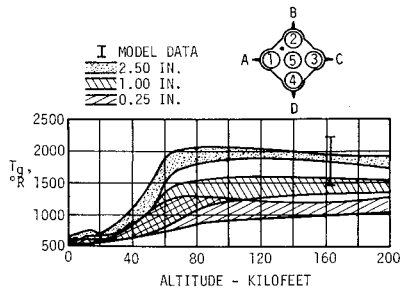

Fig. 16 Comparison of model and flight data base gas temperature.

Conclusions

1) Past experience with multiengine boosters indicated that radiation from LOX/RP-1 exhaust gases diminished with increase in altitude and that convective heating increased with altitude because of plume-plume interactions. In contrast, Saturn V data have indicated that significant radiation is contributed by hot gases being recirculated into the base and that peak radiation occured on the S-IC stage at 60 to 80 kft.

2) S-IC base TV camera data on the AS-502 indicated that hot gas recirculation is probably the main cause of this "radiation hump." The TV data show hot gases reaching the base heat shield at an altitude of approximately 40 kft, which correlates with the rise in the radiation heating rates.

3) Maximum heating rates of 22 and 32 Btu/ft²sec were measured on the heat shield and engines, respectively. Radiation was the main source of heating, although convective heating on the engine nozzle extensions was significant at the lower altitudes. Maximum base heat shield and engine gas temperatures of 2100°R and 2700°R, respectively, were experienced. The hot gases have the potential to produce the measured radiation heating.

4) Base flow deflectors, which scooped air into the base region on the AS-501 flight, were removed for the AS-502 flight. As a result, there was a significant increase in the AS-502 base heating. Radiation from the recirculated exhaust gases was the heating mechanism most affected by the flow deflectors.

5) Comparison of $\frac{1}{45}$-scale model data with flight data showed that base pressures and gas temperatures agreed reasonably well, but magnitudes of convective or radiation heating did not.

6) The S-IC heat shield and engine insulation were adequate. The base TV cameras on the AS-502 vehicle indicated that the M-31 insulation on the heat shield was cracking and pieces were falling from the base, but the resulting local increases in structural temperatures were not prohibitive.

References

[1] Payne, R. G. and Jones, I. P., "Summary of Saturn I Base Thermal Environment," *Journal of Spacecraft and Rockets*, Vol. 3, No. 4, April 1966, pp. 489–497.

[2] Krausse, S. C., "Aerothermodynamics Flight Evaluation Saturn V, AS-501," Rept. D5-15556-1, Jan. 1968, The Boeing Co., Huntsville, Ala.

[3] Krausse, S. C., "Aerothermodynamics Flight Evaluation Saturn V, AS-502," Rept. D5-15556-2, July 1968, The Boeing Co., Huntsville, Ala.

[4] Rall, D. R., "Qualification Test Report—Radiation Heat Calorimeter Model R-2030-A-22," Rept. 64-282, Oct. 1964, Hy-Cal Engineering, Santa Fe Springs, Calif.

[5] Rall, D. R., "Qualification Test Report—Total Heat Calorimeter Model C-1147-A-ZZ," Rept. 64-182, Oct. 1964, Hy-Cal Engineering, Santa Fe Springs, Calif.

[6] Malone, E. W., "Heat Flux Measurements," Rept. D2-35057, Jan. 1968, The Boeing Co., Seattle, Wash.

[7] McMillen, G. C., "Flight Data Conditioning Processes—Analytical Methods and Functional Procedures," Rept. D5-15278 A, Feb. 1967, The Boeing Co., Huntsville, Ala.

[8] Huffaker, R. M. and Dash, M. J., "A General Program for the Calculation of Radiation from an Inhomogeneous, Nonisobaric, Nonisothermal Rocket Exhaust Plume," TM X-53622, June 1967, NASA.

[9] Hendershot, K. C., "Some Observations on Exhaust Recirculation from Clustered Rocket Nozzles," AIAA Paper 66-681, Colorado Springs, Colo., June 1966.

[10] McEntire, J. A., Mullen, C. R., Jr., and Fowler, J. D., Jr., "Saturn V Model Base Heating Test Analysis (S-IC Stage)," Rept. D5-15615, Vol. 1, Aug. 1966; Vol. 2, Oct. 1966, The Boeing Co., Huntsville, Ala.